Developing fibre optic Raman probes for applications in clinical spectroscopy

Oliver Stevens[a], Ingeborg E. Iping Petterson [a,b], John Day [a], Nick Stone[b,c]

Raman spectroscopy has been shown by various groups over the last two decades to have significant capability in discriminating disease states in bodily fluids, cells and tissues. Recent development in instrumentation, optics and manufacturing approaches has facilitated the design and demonstration of various novel *in vivo* probes, which have applicability for myriad of applications. This review focusses on key considerations and recommendations for application specific clinical Raman probe design and construction. Raman probes can be utilised as clinical tools able to provide rapid, non-invasive, real-time molecular analysis of disease specific changes in tissues. Clearly the target tissue location, the significiance of spectral changes with disease and the possible access routes to the region of interest will vary for each clinical application considered. This review provides insight into design and construction considerations, including suitable probe designs and manufacturing materials compatible with Raman spectroscopy.

Introduction

This review provides an overview of various clinical applications of Raman probes to date. This is followed by a discussion of key considerations for the design and use of biomedical Raman fibre probes for clinical application. There have been a number of recent review articles detailing various optical design options[1,2], these are only briefly covered in this article. Here we focus predominantly on critical design considerations for optimising Raman probe performance for specific clinical applications.

Raman spectroscopy

Raman spectroscopy has been demonstrated by numerous research groups to be a powerful tool for molecular analysis of disease[3,4,5]. The technique relies upon the phenomenon of inelastic scattering of laser light by molecules in the sample volume [6]. The shift in energy of the scattered light is specific to the vibrational modes of the molecules composing the cells and tissues of interest. As the technique relies upon light to probe disease specific molecular changes, it can be applied non-invasively, particularly where fibre optic access is possible. The molecular information obtained can be used for the discrimination of cell and tissue types, and diseased versus healthy tissues[7]. Raman spectroscopy based instruments have the potential to provide, rapid, objective, minimally-invasive tools for use in the clinic; that are able to provide discrimination that matches and even surpasses gold standard techniques[8].

Biochemical changes in cells and tissues are a result of epigenetic changes leading to a modified phenotypic expression of the cell. These changes can often precede a morphological changes used by pathologists for disease discrimination. Individual cells of similar origin, such as prostate cancer cells can be separated into cell line heritage and their associated susceptibility to androgen stimulus.[9]

Identifying disease specific molecular changes using inelastically scattered light from cells and tissues often requires multivariate techniques, such as linear discriminant analysis, partial least squares discriminant analysis or support vector macjines.[10,11] The changes observed are usually subtle variations in the relative concentrations of proteins, lipids, carbohydrates, nucleic acids and amino acids. Changes in protein conformations and lipid saturation can also be markers for disease states.

Malignancy associated changes can also be probed using these techniques. Crow et al. showed bladder cancer surface measurements were indicative of the stage as well as grade of disease, ie the level of invasion into the surrounding organ as well as the cancerous nature if the individuals cells being probed.[12] Leiber et al., showed in organotypic skin tissue raft cultures that Raman could distinguish the presence of sarcoma fibroblast cells in regions adjacent to the sampled volume, when compared to normal fibroblast cells.[13] Furthermore, Singh et al. demonstrated malignancy associated changes in the buccal mucosa probed by Raman in at risk patient groups from tobacco exposure.[14]

Although Raman has good chemical specificity, it is hindered by the low probability of an inelastic scattering event. From one million photons interacting with a molecule, there may only be one photon that is inelastically scattered. Furthermore, at visible illumination wavelengths many biomolecules exhibit fluorescence that can dominate the weaker Raman signal. This can be minimised by using near infrared (NIR) illumination, which is usually insufficient to induce electronic absorption. However, using longer wavelengths (λ) of light reduces the inelastic scattering cross-section, which is proportional to λ^{-4}.

Accurately measuring these relatively small signals from biological tissues *in vivo* creates a technical challenge. Each application within the body imposes its own design constraints on the probe, to ensure optimum delivery of the excitation light and the efficient collection of the inelastically scattered light. This has led to the development of various different Raman spectroscopy-based probe instruments for *in vivo* use. In general, such probes must be relatively small, yet still provide spectra of sufficient quality in a reasonably short measurement time. Additionally, the probes must meet the specific requirements for *in vivo* clinical use such as being constructed of biocompatible, non-toxic materials and be sterilisable. In this paper we provide an overview of different probe design features as well as manufacturing processes that enable Raman probe instruments to be tailored to specific clinical / biomedical needs. Table 1 provides an overview of many of the Raman probes developed and utilised for biomedical applications to date. Key features of these probes will be discussed throughout this paper.

Table 1: Summary of Raman probes and applications.

Probe	Main design features	Medical Applications	Citations
Hollow Waveguides	No fibres - minimised background	N/A	Miyagi and Kawakami, 1984[15] Miyagi, 1985[16] Komachi et al., 2005[17] Komachi et al., 2005[18]
Optical fibre low background	Optimised probe for SERS to reduce Raman background	N/A	Ma and Li, 1994[19] Ma and Li, 1996[20]
Envivia (Visionex)	Inline filters in tip to reduce silica signal interference	Measurement of various ex vivo tissues	Shim and Wilson, 1997[21] Shim et al., 1999[22]
Cervical probe	Fibre optic bundle with inline filters (12mm diameter)	Normal and precancerous cervical tissue *in vivo*	Mahadevan-Jansen et al., 1998[23]
Optical fibre probe	1.75mm ball lens probe	Normal and malignant breast tissue	Motz *et al*, 2004[24]
Fibre optic array probe	Spatially offset, circular array of fibres	Measurement of bone spectra (rat and chicken) through skin	M.V. Schulmerich, et al., 2006[25] M.V.Schulmerich, et al., 2006[26]
Inverse SORS probe	Illumination ring for minimal photo bleaching and depth measurements	Deep Raman (subsurface)	Matousek, 2006[27]
Micro Raman probe	Micro Raman endoscope	Rat Esophagus and Stomach *in vivo*	Hattori et al., 2007[28]
Micro esophageal endoscope	Confocal, sub-mm diameter	Human Barrett's oesophagus *ex vivo,* Oesophageal cancer	Day et al., 2009[29] Kendall, et al., 2010[30] Almond, et al., 2012[31]
EMvision/ EMvision Miniprobe	6 fibres for collection around 1 for illumination. Filtration by coated fibres and lensing for beam steering.	Human brain cancers *in vivo* (surgery); (rabbit) atherosclerotic plaque depositions *in vivo;* Lung cancer *ex vivo*	Magee et al., 2009[32] Matthäus et al, 2012[33] Sharma et al., 2014[34] J.Deroches et al., 2015[35] Agenant et al., 2014[36] M. Jermyn et al., 2015[37]
SORS probe with multiple offsets	Consecutive rows of collection fibres with SORS spacing from excitation fibre	Human soft tissue layer discrimination and breast Tumour margins *ex vivo*	Keller et al., 2009[38] Keller et al., 2011[39]
High-axial resolution hollow waveguide probe	Hollow waveguide with ball lens	Stomach *ex vivo* (mice)	Katagiri et al., 2009[40]
Contact fibre-optic probe	Trans cutaneous measurements	Trans cutaneous musculoskeletal tissues in human cadavers	Esmonde-White et.al, 2010[41]
Flexible silicone 360^{o} probe	Silicone band with plug-in 360^{o} collection and excitation fibres	(Mice)Bone *in vivo*, *ex vivo*	Okagbare et al., 2010[42]
Beveled multi-fibre-tip probe	Beveled with ball lens tip and in line filters	Dysplasia in human Barrett's oesophagus *in vivo* real time	Bergholt et al., 2011[43] Wang et al, 2013[44] Bergholt et al., 2014[45]
Multicore fibre with integrated fibre Bragg gratings	Potential to be semi-disposable Bragg gratings	(Porcine) Brain tissue *ex vivo*	Dochow et al., 2012[46]

Photonic crystal fibre probe	Kagome hollow core photonic crystal fibre, potentially disposable	N/A	Konorov et al. 2006[47] P. Ghenuche et al., 2012[48]
Probe with polymer cap	Built in calibration due to fluorocarbon probe tip	Rat tibia	Okagbare and Morris, 2012[49]
2-fibre subcutaneous needle probe	Bevelled tip , inside hypodermic needle, sub-mm diameter	Human lymph nodes *ex vivo*	Day and Stone, 2013[50]
Kaiser PhAT probe	Commercially available 6 mm laser spot size for volume measurements	Bone *ex vivo* Joint tissues Bone *in vivo* in surgery non-invasive through skin	Esmonde-White and Morris, 2013[51] Kosi.com[52]
Endoscopic probe with shallow depth of field	Ball lens for shallow depth of field	In-vivo measurement of gastric dysplasia	Huang et al. 2010[53] Mo et al. 2010[54]
Hollow waveguide brain probe	no fibres – Hollow needle	Brain tissue *ex vivo*	Stevens et al., 2014[55]
Iris- SORS probe	adjustable SORS offset	proof of principle in phantoms and model systems	Wang et al., 2014[56]
Multi-fibre needle probe	Inside sub-mm hypodermic needle, disposable tip with non-filtered distil fibre, autoclavable	human lymph nodes *ex vivo*	Iping Petterson et al., 2015[57]

Clinical application of Raman probes

Numerous groups have explored the use of Raman probes for clinical applications over the last 20 years. These have been explored for *ex vivo* point of care testing to *in vivo* analysis of superficial lesions such as skin and epithelial surfaces using endoscopic probes to *in vivo* analysis of tissues in open surgical field such as the breast and brain. A brief overview is given here to provide the context for the design considerations that follow.

Intra-operative surgical applications

Breast cancer surgery often requires intraoperative analysis of tissues to ensure clear tumour margins are removed and that any local invasion into surrounding lymph nodes is identified and treated appropriately. The feasibility of using Raman spectroscopy for intra-operative assessment of the sentinel axillary lymph nodes during breast cancer surgery has been explored[58] Horsnell et al. utilised a commercially available portable spectrometer and large handheld probe MiniRam II (B&W Tek, Newark, DE, USA) to demonstrate the ability to discriminate normal and metastatic lymph nodes using multivariate classification models, achieving 85-92% sensitivity and 88-100% specificity in a leave-one-out cross-validation This device incorporates a 785nm laser with a spot size of 85µm and a maximum power of 300mW at the probe tip.[59] In this study only single points within the lymph nodes were probed. Minor improvements in sampling may improve results further.

Raman spectroscopy has also been proposed for detection of tumour margins during breast cancer surgery, both in-vivo and ex-vivo.

A hand-held Raman probe was developed for in-vivo collection of single-point Raman spectra during surgery.[60] The authors measured 30 Raman spectra from nine patients: 29 from margins subsequently found to be negative on pathology examination (21 were composed of normal breast tissue whereas 8 contained fibrocystic change) and 1 spectrum from a margin subsequently found to be positive on pathology examination (high-grade ductal carcinoma in-situ). Although only one malignant sample was included, this study showed the potential for in-vivo diagnosis of margins during surgery. Alternatively, confirming negative resection margins can be achieved by analysing the surface of the resection specimen ex-vivo.

Keller et al.[38] performed a conceptual study applying spatially offset Raman spectroscopy (SORS)[61] to the identification of soft tissue lesions ex vivo at depths of several mm's. Further improvement of the SORS geometry in this application enabled sample characterisation up to depths of 2 mm.[39] A probabilistic scheme was used to classify the composite spectra as 'negative' or 'positive' margins. The discrimination achieved 95% sensitivity and 100% specificity, when tested using a leave-one-out methodology.

In the brain, Koljenovic et al. showed that fibre-optic Raman probes based on the high-wavenumber spectral region (2400 – 3800 cm^{-1}) can be used to characterise porcine brain tissue ex-vivo.[62] The measurement of the high-wavenumber spectral region avoids the background Raman scattering from silica fibres while still providing high-chemical specificity and diagnostic power.[63,64] The authors developed multivariate classification model (least-squares fitting) that allowed discrimination of brain structures based on the biochemical contrast. The Raman spectra of gray matter was characterized by high intensity bands associated to proteins, DNA, and phosphatidylcholine compared with white matter, while the spectra of white matter was dominated by spectral features corresponding to cholesterol, sphingomyelin, and galactocerebroside.

In vivo tissue analysis

Preliminary work by Lieber et al using Raman spectroscopy on the skin, indicated high-diagnosis accuracy for non-melanoma skin cancers: 100% sensitivity and 91% specificity for discriminating tumours from normal skin.[65] More recently, Lui et al developed an optimised hand-help Raman probe that allowed real-time (less than 1 second) in-vivo diagnostic.[66] This large study (more than 1000 cases of skin cancers and other skin diseases) showed that it is possible to distinguish malignant and premalignant from benign lesions, melanomas from benign pigmented skin lesions, and melanomas from seborrheic keratoses, with sensitivities between 95% and 99%, although specificities range between 15% and 54%.[66]

In 1998, Mahadevan-Jansen et al. published in vivo results using a fibre-optic Raman probe to analyse dysplastic change in cervical tissue.[23] Silica-silica fibres were shown to cause less signal disruption than sapphire and liquid guide fibres despite their tendency to generate significant background signal at low wavenumbers (below 900 cm^{-1}). The probe consisted of a single excitation fibre and 50 collection fibres and had a total diameter of 12 mm. The excitation fibre was positioned at the edge of the probe, and the laser output (at 789 nm) was reflected by a gold mirror at an angle to produce a 900 µm diameter excitation spot on the tissue surface. A bandpass filter on the distal tip of the excitation fibre blocked fluorescence and Raman scattering generated by the fibre, but transmitted the excitation light. Although demonstrating that Raman spectra could feasibly be measured in vivo using a fibre-optic, the dimensions of this probe and the time taken for spectral acquisition (90 s) meant this design was impractical for endoscopic use in other organs.

Endoscopic diagnostic applications

To enable access to other epithelial surfaces, where around 80% of cancers originate, it is important to produce a miniature probe that is compatible for use with a medical endoscope. A gastric-endoscope is typically 90 cm in length with instrument channels of around 2.8 mm diameter, through which a Raman probe could be delivered. This presents a considerable technical challenge; to package a probe with all its constituent parts (filters, collimating lenses, illumination and collection channels, and external casing) into a durable device with a diameter smaller than 2.8mm.

In 1999 Shim et. al. utilised an endoscope compatible, fibre-optic Raman probe consisting of one central delivery fibre (400 µm diameter) surrounded by seven collection fibres each with a 300µm diameter (Visionex probe).[22] Filters were placed over the fibres approximately 2.5 cm from the probe tip and the collection fibres were part bevelled so that they predominantly collected signal from a zone in front of the delivery fibre and at a specified collection depth, determined by the bevelled angle. This design provided a means of controlling the sampling volume whilst optimising collection efficiency.

In 2000, Shim et. al. reported the first in vivo Raman measurement of gastrointestinal tissue using the Visionex probe.[67] In this feasibility study the probe was passed through an endoscope into the oesophagus, stomach and colon. Twenty patients successfully underwent the endoscopic procedure following routine sedation and no complications were reported. The probe was positioned to touch an area of mucosa for 5 seconds during which time readings were taken. The probed site was then biopsied to allow comparison of Raman spectra with histopathology at that site. Subtle differences were reported in spectra from normal and diseased areas but the data acquired was not sufficient to discriminate between pathological groups. Whilst demonstrating feasibility, Shim et al. concluded that more work was needed to enhance the SNR, to minimise acquisition times, and to improve data interpretation before reliable results could be generated. This study illustrated that endoscopic Raman spectroscopy could be performed safely in human patients, but was not large enough to enable comparison with results generated using laboratory based Raman spectrometers.

Motz et al. used a novel probe to study dysplasia in rat palate tissue using 100mW of laser light (at 830 nm) for excitation.[68] Multivariate analysis demonstrated differences in low and high grade dysplasia, but it was concluded that further modifications to the probe were necessary to optimise collection depth as a significant spectral contribution was collected from tissue that was deeper than 500 µm. More recently a greater emphasis has been placed on targeted illumination of the epithelial lining of the gastrointestinal tract. Precancerous dysplasia develops in epithelial cells and, by definition, has not yet invaded deeper structures. For optimum diagnostic accuracy, probes must collect signal from the epithelial layer and minimise spectral contributions from scattering occurring in deeper tissues.

In 2005, Wilson et. al. published results of an in vivo trial in the upper gastrointestinal tract of humans. They used a probe consisting of a central delivery fibre surrounded by six 300 µm

diameter bevelled collection fibres that achieved an estimated sampling depth of 500 µm.[69] In conjunction with a 785nm diode laser and an optimised spectrometer and CCD they reported an accuracy of 87% for delineating between normal oesophageal tissue and dysplasia.

Day et. al. developed a confocal probe specifically designed for spectral measurement in the oesophagus.[29] This probe consists of a single illumination and a single collection fibre with collimating graded index (GRIN) lenses to ensure optimal optical coupling, and in built filters to exclude intrinsic signal generated within the optical cables. The single fibre, which has a small aperture, shows a high degree of selectivity for detecting spectral signal arising from the epithelium. This probe was used to interrogate oesophageal biopsy tissue in vitro with 830nm light and demonstrated that Barrett's oesophagus, dysplasia and cancer could be successfully separated with 71-88% sensitivity and 77-99% specificity.[29]
In an attempt to achieve similar depth discrimination, Huang et. al. described the use of a ball lens at the distal tip of a novel Raman probe to focus excitation light onto the epithelium and help launch scattered light into the collection fibres.[54]

Following a number of preliminary in vitro and in vivo studies in rats, Huang et al. published a series of results from in vivo trials of endoscopic Raman spectroscopy for the detection of gastric neoplasia in humans. They used a 1.8 mm diameter Raman probe consisting of 32 collection fibres surrounding a single central delivery fibre. The probe had two stages of optical filters, at its proximal and distal ends, and used 785 nm excitation. Each spectrum was acquired in 0.5 s with a laser light irradiance of 1.5 W/cm^2. In 2010 they reported a diagnostic sensitivity of 82.1% and a specificity of 95.3% for delineating malignant gastric ulcers from benign tissue.[70] In 2011, the same Raman probe system was used in the oesophagus demonstrating a sensitivity of 97.0% and a specificity of 95.2% for detecting oesophageal cancer.[43]

An in-house developed Raman probe was evaluated for ex-vivo measurements on 105 colon specimens from either biopsies or partial colectomies (41 normal specimens, 18 hyperplastic polyps and 46 adenocarcinomas) from 59 patients. With acquisition times of 5 seconds, the authors developed diagnostic algorithms that achieved a cross-validated diagnostic accuracy around 98%, although this study did not include adenomas, which are an intermediate pathological group in the stepwise progression from normal tissue to adenocarcinomas.[71]
Recently Sato et al. tested a miniature Raman-endoscope system was used to measure spectra sequentially over a period of several weeks to monitor tumour progression in 4 mice with recognisable tumour lesions. Molecular changes in the tumour as it progressed, such as altered collagen type I and lipid content were measured and they were able to classify 86.8% of samples correctly as tumour versus normal tissue, when compared to histopathology.[72]

Recent work by Short et al. has examined the possible use of high frequency Raman in the colon, measuring wavenumbers in the range 2050 to 3100 cm^{-1}.[73] Although discriminatory peaks were mostly detected at lower wavenumbers, measuring in this higher range reduces the effects of tissue auto-fluorescence and emissions in the fibre-optic probe itself. This means that cheaper probes can be produced without the need to filter the light within the probe. This small study in ex vivo fresh colonic tissue samples has shown that discrimination of pathology subtypes is possible using these higher wavenumbers with 1 second acquisition times.

Much work in the oesophagus has been aimed at the development of a fibre-optic Raman probe for in vivo use, designed to be compatible with medical endoscopes. Initial work in rats models in-vitro showed potential for in vivo applications.[74] Safety and feasibility of using Raman probes in the oesophagus was shown using an Enviva Visionex probe. 400 spectra in 20 patients were measured using 5 second acquisition times, although discrimination of pathology was poor[67] due to large sampling depths. This was followed up with a custom-built probe which was used to discriminate Barrett's, low-grade dysplasia (LGD) and high-grade dysplasia (HGD)/adenocarcinoma with accuracy 88%, 81% and 92% respectively in 192 spectra from 65 patients with Barrett's oesophagus using 5 second acquisition times.[75]
Elsewhere, in vivo diagnosis of oesophageal cancer with Raman fibre-optic probes has been reported with sensitivity 91% and specificity 94%, although subtype of cancer or degrees of dysplastic change were not differentiated. This study measured 263 oesophageal Raman spectra from 80 patients (33 with cancer) with relatively fast acquisition times of 0.4–0.5 seconds.[43,76]

Utilisation of a confocal Raman probe has been shown to provide accurate recognition of pathology subtypes using spectra acquired in 1 second using a Raman probe, giving sensitivities and specificities for normal squamous of 87% and 96% respectively, Barrett's/LGD 72% and 91%, HGD/ adenocarcinoma 86% and 88%.[77]

Seven hundred and ninety-eight, 1 second Raman probe spectra were acquired from 673 oesophageal tissue samples from 62 patients. 5 second and 0.1 second spectra were also recorded for comparison. Principal component fed linear discriminant analysis was used to calculate probe accuracy by reference to a consensus histopathological 'gold standard' diagnosis. All results were statistically cross validated, based on characteristic spectral signatures. High-grade dysplasia and adenocarcinoma could be discriminated from Barrett's oesophagus, low-grade dysplasia and normal squamous oesophagus with a sensitivity of 86% and a specificity of 88%. The ability to detect early superficial mucosal disease, including discrimination between low-grade and high-grade dysplasia, was also demonstrated despite short, clinically applicable (1 second) spectral acquisition times. However, enhanced diagnostic accuracy was demonstrated when using 5

s acquisition times; the detection rate of HGD/ adenocarcinoma remained 86%, but the specificity was greatly improved at 98%.[77]

In addition, a potential algorithm for multi-system spectral classification was defined and consistent measurements were recorded by two independent operators using two identically built probes. The potential for bimodal diagnosis using a combination of RS and narrow band imaging was also demonstrated. No single incident of thermal tissue injury was reported.[11]

The first use of Raman fibre probe based analysis in the bladder was performed by Crow et al. using frozen tissues.[78] A Visionex probe was used for this work at 785 nm and although the background signals from the probe were found to be significant there were still sufficient pathology specific signals to enable discrimination between 220 Raman spectra from 29 snap-frozen bladder samples from benign (normal and cystitis) and malignant samples (transitional cell carcinoma), with an overall accuracy of 84%. However, the probe design required filters and expensive manufactured tips to minimise contributions from the signals induced in the fused silica core of the fibres. An alternative approach is to use the high wave number region (2400—3800 cm^{-1}), where silica has no Raman signal. This enables the use of a single unfiltered fibre to guide laser light to the tissue and to collect scattered light in this spectral region. Koljenoví c et al. showed using in vitro Raman microspectroscopy on bladder tissue that both the fingerprint and high wavenumber regions contained similar levels of diagnostic information. Thus indicating simple fibre optics and the high wavenumber region may be sufficient for many applications.[64]

The first in vivo bladder Raman studies using an Emvision probe based around a filtered six collection fibres around one illumination fibre.[79] They used the fingerprint region and 785nm illumination. The probes had no lenses or beam steering and this meant that signals were collected from both the urothelial surface of the bladder and the deeper layers, thus diluting the key diagnostic signals for early disease. Spectra were obtained from suspicious and non-suspicious bladder locations during the procedure of transurethral resection of bladder tumours (TURBT) with collection times of 1—5 s. Multivariate analysis was used to generate the classification models. The algorithm was able to distinguish bladder cancer from normal bladder locations with a sensitivity of 85% and a specificity of 79%. The results show the possibility of discerning normal from malignant bladder tissue by means of Raman spectroscopy using a small fibre based system. Despite the low number of samples the results indicate that it might be possible to use this technique to grade identified bladder wall lesions during endoscopy.

Integration into the clinical workflow

Various attempts have been made to couple Raman with other modalities to maximise its potential for clinical impact. This section outlines a few examples.

The feasibility of combining wide field imaging techniques with Raman probes for specific disease detection in the lung was investigated for pre-neoplastic lesions in-vivo, by integrating Raman spectroscopy measurements to a bronchoscope based on white light and autofluorescence.[80] White light and autofluorescence images allowed identification of suspicious lesions, areas from which Raman spectra were measured with acquisition times of 1 second. The authors showed that sensitivity of 96% and a specificity of 91% for discrimination of pre-neoplastic lesions (leave-one-out cross validations) by developing multivariate statistical models.

Fluorescence guided endoscopy (FGE) has been proposed as a guidance tool to improve early detection in diagnosis and complete removal of superficial transitional cell carcinoma during surgery. There is a great deal of evidence to demonstrate the benefits of the use of ALA-fluorescence cystoscopy for the identification of malignant lesions invisible at white light cystoscopy.[81] The accumulation of PpIX, a precursor of heme, within abnormal cells enables these areas to be identified because they fluoresce red when illuminated with blue light. However several studies have demonstrated the low specificity of fluorescence imaging. Combining fluorescence with Raman spectroscopy in a multi-modal approach could improve its diagnostic capability. Optical biopsy by means of Raman spectroscopy at the region of interest selected by fluorescence imaging may enhance specificity and provide in vivo pathology.[79,81] A major limitation in its clinical application is the weak nature of the Raman signal, which inhibits scanning large surface areas of tissues.

In bladder cancer diagnosis, fluorescence-guided endoscopy with 5-aminolevulinic acid (5-ALA) has gained interest as a technique that can provide such spatial differentiation, thus improving early detection and more complete removal of superficial tumours. However, little is known about the effect of agents such as 5-ALA on Raman spectra of tissue. In samples with 5-ALA, an overall decrease in Raman intensity was observed when compared to the Raman spectra from samples without 5-ALA. Additionally, differences in relative intensities at 1270 and 1330cm^{-1} were also noted.[81] However, significant differences were observed in the Raman spectra of benign and malignant samples with 5-ALA indicating the potential of using Raman spectroscopy for discriminating bladder cancer in the presence of 5-ALA.

Another example of fluorescence-Raman diagnostics has been demonstrated in skin cancers.[82] A more advanced system explored by Dochow et al., utilised a dual modality fibre optic probe combining fluorescence lifetime imaging (FLIm) and Raman spectroscopy for in vivo endoscopic applications. This was tested on various animal tissue samples and appeared to be able to provide signals from both modalitites to distinguish tissue types. There maybe some risks associated with the use

of short wavelength excitation of the FLIm signals. A risk / benefit analysis may show this to be of overall benefit to the patient.[83]

One further demonstration of real-world clinical translation has been demonstrated by Desroche et al.[35] and Le Blond et al.[36] They have integrated a neuro-navigation attachment on the probe to allow co-registration with preoperative MR images. A further advancement for prostate cancer surgery by Nyberg et al.[84] have shown that Raman spectroscopic probes can be combined with tactile resonance approaches to provide surgeons with 'feel' and biochemistry of prostate tissues.

Key clinical Raman probe characteristics

Size

Small Raman probes are often desirable, as they enable new applications that cannot be addressed by larger probes. Miniaturisation comes with a cost however, particularly in terms of collection efficiency, and design options are far more limited at smaller sizes. The Raman probes demonstrated to date can be broadly separated into three size classes (Table 2).

Table 2. Small fibre optic based probes have been designed for different medical applications.

Probe diameter	Application	Design constraints	Signal Performance
cm	Portable analysis outside body, e.g. skin	Low, most optical designs possible	Very high
mm	Endoscope: hollow organs	Moderate, many optical designs possible but challenging	High
sub-mm	Below skin, Solid organs	Optical designs very limited, even basic lenses difficult to include	Moderate

The largest class of probe generally has diameters around the centimetre scale. Such probes are essentially handheld. There are a good number of commercially available probes at this size, there are few limits on the designs possible, and throughput and Raman collection performance is typically excellent. These probes can often achieve similar performance in terms of signal per mW per cm^{-1} as achieved with a microscope based system. These types of probes are usually used on skin, accessible organs, or exposed parts of the body during surgery.[85]

At the millimetre scale construction becomes more difficult, especially if good optical alignment is required. Although bespoke commercial manufacture is becoming more widely available, most probes of this size range have been produced by research groups. Filters and lenses can be incorporated at this scale, but optical designs are significantly limited by space constraints. Probes within this size range are small enough to enter into the human body to inspect hollow organs, as they may fit into endoscopes, which have working channels generally of the order of 2-3 mm. Spectral performance can be very good, but is typically lower than that of larger probes and microscope based spectrometers.

Sub-millimetre probes can be utilised to penetrate beneath the skin and into solid organs, either directly as a needle probe, or into a core biopsy needle. At this size range optical designs options are severely limited and incorporation of lenses and filters can be a challenge.

Fibre optic probes

Fibre optics provide many advantages for biomedical Raman probes because they act as a flexible waveguide, directing the excitation beam to the point of interest, and they also improve the efficiency of backscattered collection by returning more collected light back to the detector.

Glass fibres

Fibre optics used for Raman spectroscopy applications are most often multi-mode fibres formed of fused silica glass (SiO_2) in a step-index format. The refractive index of the fibre core is made considerably higher than that of the cladding, by elemental doping of the silica glass, typically with elements like Fluorine, Boron or Titanium. This refractive index miss-match causes total internal reflection within the fibre core, as depicted in Figure 1. The light that enters the core is not able to escape laterally through the cladding and therefore is propagated through the fibre length. Generally, fibres are also encased in a buffer or external protective coating, made of metal or polymer that strengthens the fragile fibres. For biomedical applications utilizing NIR light, the use of low-OH silica glass is recommended to reduce OH absorption in this region of the spectrum.

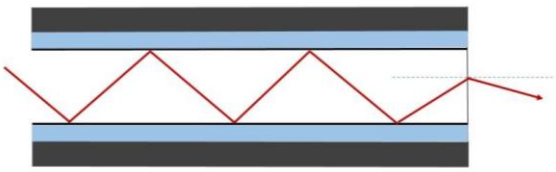

Figure 1. Schematic diagram showing total internal reflection in glass fibre optic.

Maximising throughput

The collection efficiency of a system is characterised by its étendue, which is the product of the collection area and the solid angle over which scattered light is collected by the system. The concepts of étendue and the Lagrange Invariant must be born in mind when designing a system since an ideal optical design conserves étendue along the optical path. The system is therefore ultimately limited by the étendue of the least efficient component in the system. In small systems with small working distances this is usually governed by the optical fibres or ultimately by the spectrometer itself. Spectrometers are typically specified by their f-number: defined as the ratio of the focal length to the diameter of the effective aperture of the entrance optics. Many typical Raman spectrometers have f-numbers of 2 or greater. For optical fibres the collection angle is usually specified as the Numerical Aperture (NA), which describes the illumination and collection cones produced or accepted by the fibre. NA is defined as the sine of the half angle of the collection cone. The NA of the fibres is determined by the refractive indices of the core (n_1) and cladding (n_2) of the fibre and given by

Eq.1. $$NA = \sqrt{(n_1^2 + n_2^2)}$$

Fibre optics are readily available with NA values ranging from 0.1 to 0.5. NA and f-number are related by the equation

Eq. 2 f-number = 1/(2NA)

The importance of the conservation of étendue can be shown by a simple example. A single fibre can be used for light collection at the sample and connected directly to the input aperture of a spectrometer. A large numerical aperture fibre is clearly preferable for the most efficient collection of light however a typical fibre has an N.A of 0.22 equivalent to an f-number of 2.3. Many small spectrometers have f-numbers of 3 or greater so the fibre is likely to overfill the acceptance angle of the spectrometer aperture and the spectrometer will not collect all of the light delivered by the fibre.

The use of a high NA fibre is therefore unlikely to significantly increase the system throughput and is likely to create more stray light and background problems. Similarly the use of larger fibres is an intuitively obvious step to increasing light collection however the spectral resolution of the system is determined by the width of the spectrometer entrance slit. Typical Raman systems require slit widths of around 0.1 mm, similar to a typical fibre core diameter so larger cores may be vignetted by the slit and offer no advantage or may require a larger slit and result in a decreased spectral resolution. A larger fibre may be optically de-magnified onto the slit but the resulting angular magnification will create a larger effective numerical aperture so still overfilling the spectrometer.

For these reasons it is usually preferable to increase the throughput by using multiple small fibres that can be arranged vertically along the slit width instead of a single large fibre. Some modern spectrometers are now available with entrance optics that asymmetrically image the source onto a virtual slit at the focal plane of the spectrometer so utilising the full available height of the entrance aperture and hence the maximum possible étendue of the spectrometer.[86] Whatever configuration is used the étendue is still conserved and the overall system efficiency is always governed by the least efficient component.

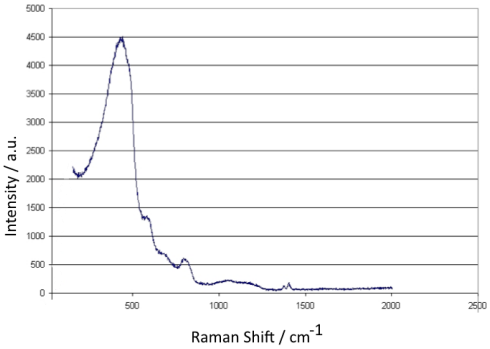

Figure 2: Raman Spectrum of Silica fibre. Note the characteristic background shape, particularly below 700cm^{-1}

Fibre background

Whilst there are clear advantages to the use of optical fibres in Raman probes, the silica that these fibres are constructed from impart an unwanted background signal onto the collected Raman spectrum. A Raman spectrum of a typical silica core fibre optic is shown in figure 2 This unwanted signal is generated in the laser delivery fibre and also by elastically scattered light entering the collection fibre.

Qualitatively this has a detrimental effect on the spectrum, adding a significant background to the spectrum and causing the appearance to differ significantly from a spectrum collected by a Raman microscope, which hinders comparative analysis. It also has a quantitative effect on the signal to noise ratio, as the additional counts from the silica only serve to increase the total number of spectral counts and the associated noise with no beneficial effect.

Reductions in silica background can have a marked effect on performance. The scattered light measured exhibits shot noise described by Poisson statistics where the noise level increases as the square root of the number of incident photons. Equation 3 shows the expression for signal to noise taking into account the signal from the sample, N_S, and the background signal from the silica, N_B. The detection limit of the desired signal is frequently determined by the shot noise present in the silica background instead of the collection efficiency of photons from the sample. This limit also becomes sample dependant as a highly reflective sample will reflect more of the excitation beam back through the probe and create a larger background.

If the silica background is equal to twice the tissue Raman signal intensity, then the signal to noise ratio can approximately be doubled by removing the silica background altogether, or avoiding the spectral regions where the silica signals reside (see Figure 3).

Eq.3 $$SNR = \frac{N_S}{\sqrt{(N_S+N_B)}}$$

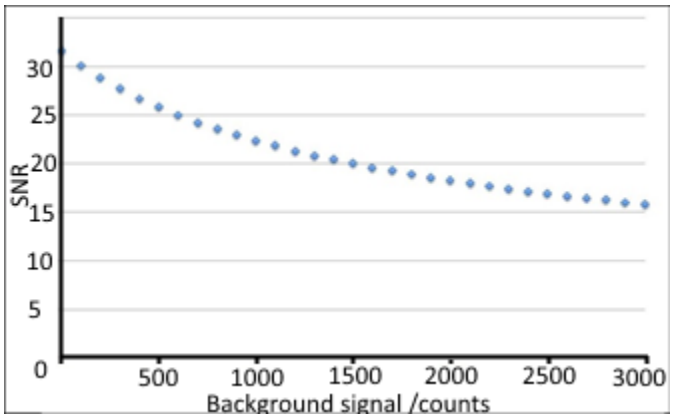

Figure 3. Signal to noise ratio versus background for fixed signal counts (N_s) of 1000.

Reducing this internal silica background is therefore an important challenge for probe designers, and also an increasingly important avenue for improvements in performance of designs that otherwise have throughput limited by spectrometer efficiency. One common reduction strategy is to ensure optical filters are placed as close as possible to the sample, to limit the length of fibre where the backscattered laser light can generate Raman signals from the probe itself. For larger probes this is straightforward, for smaller probes this can require tiny filters, or even filters coated directly onto components. In general most fibre optic probes place filters at the tip to eliminate the fibre background. This does place constraints on the design of the probe, and also makes them more expensive, potentially too expensive for single patient use. Even with state of the art filters of optical density of 6 or more, significant background still remains present in the spectrum. This silica background has been shown experimentally to increase with numerical aperture, and the length of both the collection and laser delivery fibres, though fibres carrying laser light have a larger effect.[87]

Background subtraction during post-measurement processing can improve the similarity of probe spectra to reference spectra from Raman microscopes. However, it can also introduce unwanted distortions and variability between spectra and most importantly does not improve the quantitative signal to noise performance. The shot noise introduced by the background cannot be subtracted with the overall background signal profile.

Many groups working with Raman probes have prudently avoided unwanted interference by restricting their analysis to the higher wavenumber regions of the spectrum (2800-3700 cm^{-1}).[63,88,89,90] Although the entire spectrum is affected, the silica background is most significant below around 700cm^{-1}. Some potentially useful discriminatory information is lost in ignoring the spectral features in this lower region, however with a large amount of chemical information available in the bands from 700cm^{-1} to 1800cm^{-1}, good analysis can take place despite the interference.

An alternative method has been explored for filtering the elastically scattered laser line from the collection fibres and thus minimising the induction of background signal from fibres. This uses in-line fibre Bragg gratings (FBG) to reject/reflect the laser light in the collection path. A Raman probe was built consisting of one excitation fibre and six multicore single-mode fibers (19 cores) with inscribed FBGs as collection fibres.[46]

Fibre Buffer Composition

Silica glass fibre optics are coated with a protective outer coating called a buffer or jacket that serves to add extra support and strength to the delicate fibre. These buffers may be made of various different materials; polymers or metal coatings are the most common. If a minimal total diameter of the fibres is a critical aspect of probe design, the buffers can be removed. Polymer coatings are easily removed with specialized fibre stripping tools, and this can be facilitated by soaking the fibres first in a solvent like acetone to loosen the buffer. Metal buffers can be removed by chemical etching. In all cases it must be ensured that the buffer layer does not contribute to the signal. This is particularly important for fluorescent buffers such as polyimide in which case the probe design must ensure that the buffer is not directly in the signal or collection path.

A dense, opaque coating on the fibres, such as a metal buffer, can provide an advantage in a probe where fibres are tightly packed. This coating will eliminate any cross-talk between adjacent fibres, however a buffer also increases the overall diameter of the fibres considerably, and additionally, care must be taken to use biomedically approved materials. Metal coatings of gold or stainless steel are recommended, however copper and aluminium alloys are common fibre buffer materials, which may not be biocompatible and must be used with caution in biomedical probes.

The fibre diameter, as well as total number of fibres and their packing configuration are frequently important considerations in determining the overall diameter of probes employing multiple collection fibres. These factors become increasingly critical the smaller the desired probe design, particularly for probes in the sub-mm range. Typical cladding diameters range upwards from 0.125mm with larger core sizes obviously necessitating larger fibres.

Additionally, claddings and buffers/jackets may contribute towards dead space (inactive area of the probe), which can be reduced considerably by stripping off the fibre buffer jacket, however the resultant bare fibre is extremely fragile and some additional mechanical protection will usually be required.

Hollow waveguides

An alternative strategy is to replace fibres with waveguides: hollow glass tubes internally-coated with metal mirrors. It has been shown[15,16.17,91] that this does indeed result in a lower silica background, but much higher losses than silica fibres have been reported. The diameter of these waveguides is also considerably larger than most silica fibres (0.7-1mm). Some of the flexibility of glass fibres is also lost, and manufacture is more difficult.

For larger diameters (approx. 1-2mm), it is possible to use a collimated beam of light in the distal section of the probe and in effect no waveguiding is required.[55] This is in effect a mini-stand off design and makes it possible to use hollow metal tubes / needles without the requirement for fibres or waveguides, improving medical compatibility. The lower numerical aperture of this arrangement is broadly compensated for by the larger collection area and reduced background, though the applications are more limited as the probe cannot be allowed to flex in the collimated section. Studies in our own lab indicate that this configuration has an efficiency of about 10% compared to a 0.22 NA low-OH fused silica fibre (105/125 core cladding). However the significantly reduced fibre background can give a similar signal to noise for some applications. Figure 4 demonstrates the effect on background caused by different probe geometries. The conventional microscope based Raman system clearly shows the smallest silica background as expected followed by a miniature stand off system[55] with minimal fibre use. A two-fibre needle probe and a commercially available fibre probe show the largest silica background signals

Photonic Crystal Fibres

A relatively new development is the availability of photonic crystal fibres (PCFs). In this class of fibre, light is guided in an air core, rather than in silica. In theory this implies no silica background at all, and groups that have used these fibres show large reductions in background, 10 times when the excitation fibre is replaced[47] and 100 times where PCFs are used for both excitation and collection.[48] Throughput has been shown to be much better than with metal-coated waveguides. So far the only demonstrations have been of very simple probe designs. PCFs are becoming much more readily available but remain very expensive in comparison to silica fibres, and whilst they can be designed to operate at many wavelengths they have a much narrower range of wavelengths that they will accept than silica fibres, reducing the range of Raman shifts than can be observed when used for collection as well as excitation. They also present construction difficulties, with generally small core sizes and delicate internal core structures.

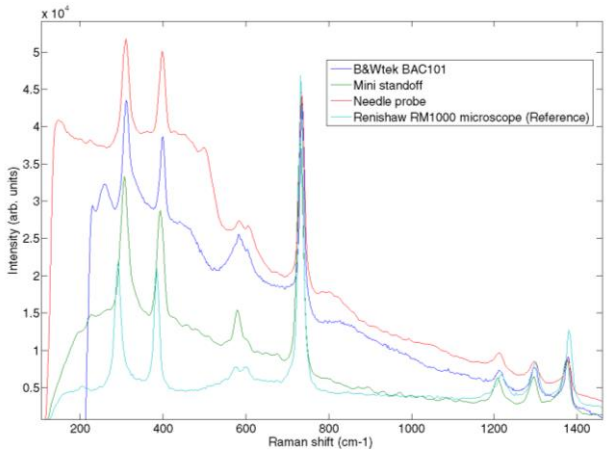

Figure 4: Spectra demonstrating differing silica backgrounds of various probe configurations.

Manufacturing materials

Utzinger and Richard-Kortum gave an overview of different manufacturing materials for biomedical probes, and their biocompatibility in 2003[2]. Since this overview, many new materials and manufacturing techniques have become available, particularly of note, the increasing availability of additive layer manufacturing, or '3D printers', capable of printing in different kinds of plastics, as well as metals. See supplementary information.

Fluorescence from other probe materials

Aside from inherent fibre background, another major culprit in spectral background contribution is the glue used to fix fibres and optics into place. Many medical-grade glues that are used to construct clinical instruments are UV-cured epoxies. These glues are not suitable for the construction of clinical Raman probes because they contain a fluorescent photo-initiator used for hardening the glue. Transparent/colourless 2-part chemical- or heat- cured epoxies are recommended for Raman probe construction.

Even if the glue is not directly in the excitation or collection path of the probe, it is possible for a small fluorescence contamination to completely overwhelm the Raman signal due to stray reflections, as shown in Figure 5.

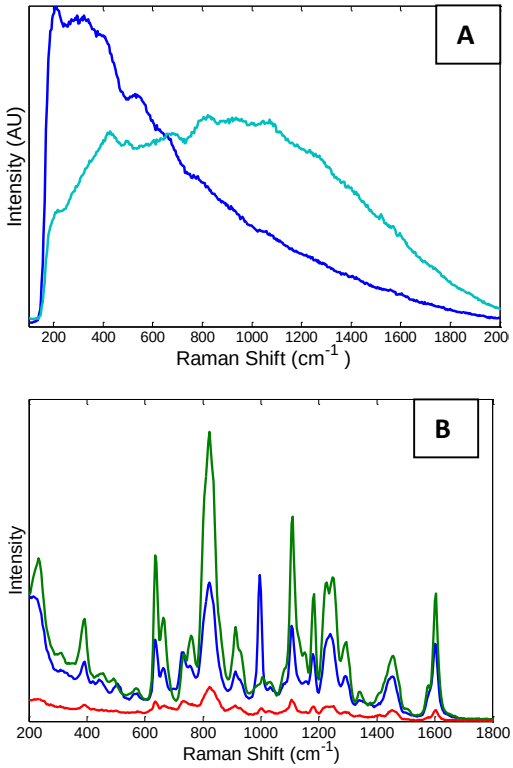

Figure 5: Raman spectra of various biomedical- approved glues. Glues with spectra shown in panel A are UV- cured and contain a fluorescent photo-initiator for hardening, and the resulting cured glue is highly fluorescent and not appropriate for use in Raman probe designs (see supplementary information). Panel B shows spectra from biomedically-approved 2-part epoxies that are colourless/transparent. Panel A uses 0.1 s acquisitions, panel B uses 1 s acquisitions, both with the same power density (Raman microscopy).

Geometry and sampling volume

With Raman scattered photons so scarce, a probe must collect as much light as possible for the best performance. It is important though to be mindful that the end goal is classification or analysis, and hence it is crucial to be careful that the collected light is from the diagnostically relevant region of the sample. Collecting more total light, but from the wrong region of a sample may reduce the clinical effectiveness of the probe. The geometry of a biomedical probe design should therefore be a major consideration, and tailored to the nature of the clinical application. The sampling volume of a probe may be varied by altering various design parameters, including fibre diameter, number of fibres, fibre NA, the angle of the probe face with respect to the optical axis, as well as through the addition of lenses or other optics at the probe tip.

Where the fibres are used at the distal tip of a probe without additional optics the fibre ends may be shaped to optimise the desired overlap between the illumination and collection regions, which in turn will affect the sampling volume. If the angle of the fibre face slopes away from the illumination cone of an adjacent fibre, this changes the area of overlap between illumination and collection angles (Figure 6). The refractive index of the sample medium also plays a key role here.

If the critical angle of total internal reflection between the fibre face and the medium is reached then the light will exit through the cylindrical side rather than the fibre face.[92,2] For a silica fibre in air this angle is 43.3 degrees and in water this is 66 degrees. For tissue this angle is around 69 degrees (for n_{glass} = 1.5 and n_{tissue} = 1.4). However, probes are not always fully submerged into tissue and an air gap can exist between the probe tip and sample surface.

If the angle slopes towards the illumination cone this can create a smaller acceptance angle and thereby a shallower sampling into the medium. A common probe design that utilizes this design feature is to create a beveled tip on the probe face, which significantly changes the angle of illumination and collection towards a shallower collection volume. See Figure 6.

Depth selectivity

A number of biomedical Raman designs incorporate some form of 'depth selectivity', as an attempt to minimise collection of light from deeper regions within the sample, or collecting relatively more light from shallower regions of a sample. See table 3. This is of great importance in some applications. Examples include, diagnostic tools for skin and for epithelial cancers on the lining of organs such as the bladder, colon and oesophagus, whereby the dysplastic cells of interest are often in a very thin surface layer on the inner surface of the oesophagus, and a surface measurement is required to probe the cells of interest [60].

Bevelled tips

The simplest method of achieving some depth selectivity is to use a bevelled tip of the distal fibres. This method is favoured for its simplicity and use in smaller probes where other options are limited. This approach has been implemented in a two-fibre design[50] or as a ring of collection fibres around a central excitation fibre.[94] An in-depth overview of the effect on fibre acceptance and exiting angle of different fibre face angles is provided by Utzinger and Richards-Kortum 2003.[2]

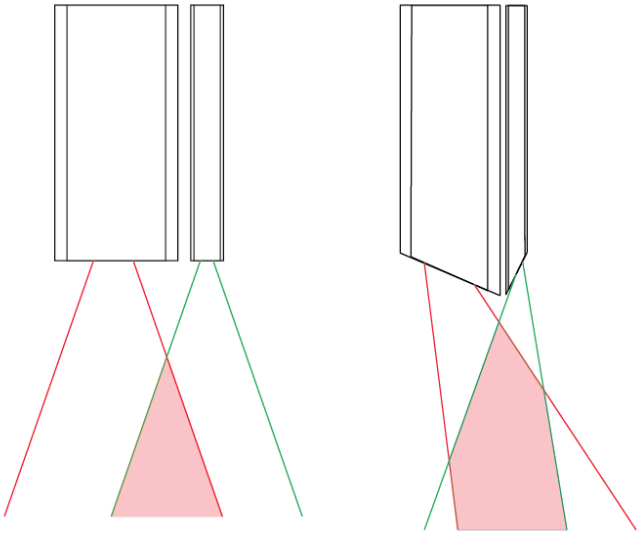

Figure 6: Demonstration of effect of geometric fibre shaping on collection volumes.

For diagnostic scenarios where deeper or bulk sampling of tissue is required on the scale of a few mm subsurface, a flat-face probe design, with separate illumination and collection fibres, is likely to be most amenable. See section on subsurface probes.

Ball lenses

There have been various probe designs that have involved utilisation of a ball lens at the tip of the probe. This serves to change the excitation and collection optical paths of the probe, as well as to provide protection for the probe tip. Choice of an appropriate lens can control the sampling volume. Using a ball lens offers a further improvement in depth selection over a bevelled tip, but is more complex to manufacture.

The ball lens also creates a distance between the fibres and the sample, often referred to as the sample-probe gap, which can be controlled by the size of the ball lens and provides a critical distance between the fibre faces and sample for obtaining maximum signal collection (see Figure 7).[95]

Confocal probes

The strongest depth selectivity is achieved with a true confocal optical layout. This produces extremely strong rejection of signals outside of the shallowest region of the sample, at some cost to total throughput. Construction of such probes is complex, as it requires very careful alignment of the components.[29] Techniques such as utilisation of silicon v-

grooves and 3D printing of optical scaffold mounds for mm scale probes have been utilised to date.

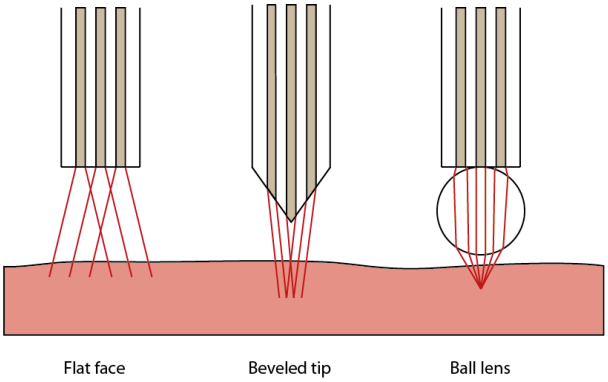

Figure 7: illustration of the basic geometries of a probe with a flat face, a bevelled tip and with a ball lens.

Subsurface probes and applications

In some biomedical diagnostic scenarios, the tissue target of interest is not easily accessible from outside the body or even via orifices and hollow organs, but requires measurements through solid tissues deeper within the body.

Spatially Offset Raman Spectroscopy (SORS) Spatially Offset Raman Spectroscopy (SORS) can be implemented if deeper subsurface sampling is required (cm + scale), or if a surface/sub-surface differential signal measurement is required. This relies upon the phenomenon first identified by Matousek and Morris, that increasing the spatial separation of the illumination and collection points leads to average Raman signal collection from greater depths.[96] This is ideal for non-invasive probing deep into samples (for example beneath skin) without invasive penetration.[39,61,96,97] Collection over such a large region of a sample has its cost however, with reduced signal to noise and a reduction in spatial resolution.

The sampling depth in tissues increases by the order of 1 mm for every 2 mm of spatial offset between excitation and collection spots.[39,96,98] In combination with this of course the volume of tissue sampled also increases and the depth resolution of the measurement decreases due to the diffuse scattering of light in tissues.

Variants on the SORS design include inverse SORS,[27] where the illumination is delivered in a diffuse ring offset from a central collection area. Inverse SORS provides bulk sampling, and in spreading excitation photons over a larger sample area potential photodamage of the sample is reduced.

Some applications of SORS probes for large tissue volume sampling include the study of disease specific, bone tissue chemistry relating to various disorders and diseases and injury,[99] as well as instruments that are under development for detection of breast cancer, prostate cancer.[100,101,102]

In the investigation of tumour margins during surgery, it is also important to discriminate any buried tumour tissue beneath the surface of an apparently normal tissue margin.[65,103]

Table 3. Sampling depth provided by different probe designs.

Sampling depth (approx.)	**Designs**	**Example references:**
10s-100s um	Confocal Lensed tip	Day et al. [29] Huang et al. [53]
mm	Lensed tip beveled tip flat face tip	Jaillon et al. [95] Hattori et al. [28] Komachi et al. [91]
cm	Large laser spot SORS Deep Raman	Kaiser phat probe[52] Matousek et al. [96] Buckley et al. [99]

Imaging probes

Raman probes that collect spatial as well as spectral information are highly desirable for biomedical applications. This has been possible using Raman microscopes for some time.

Building Raman probes with this capability is much more difficult. Most probes that have been demonstrated have fallen into two categories. The first is a multi-fibre version of a single point Raman probe. CCD based spectrometers can capture spectra from multiple channels at once, which allows an image to be constructed. This approach captures spectra comparable to single point Raman probes, but with very limited spatial resolution.

Another approach is to use a coherent fibre bundle to capture information with a high spatial resolution, and use a wavelength selective filter instead of a spectrometer. This has been demonstrated with acousto-optical-tunable-filters (AOTFs)[104] and liquid crystal tunable filters (LCTFs).[105,106] Both approaches have very low spectral resolution, typically too low for effective use in discriminating subtle differences in pathology. LCTF filters can be constructed with sub-nm resolution, but such filters would be extremely expensive and have very low throughput. Acquisition times are also likely to be prohibitively long, as Raman signal must be collected consecutively from each band of interest.

Choice of laser wavelength

Near infrared wavelengths in the range 785-830nm have been demonstrated to be the optimum choice for minimising fluorescence backgrounds in biological tissues while still allowing the measurement of the Raman scattered signals with silicon CCD dectectors.[107]

Dealing with biological contaminations

A major consideration in the design of biomedical probes is in minimizing soiling of the probe from biological tissues and fluids, as well as preventing cross contamination in multiple uses for different patients. Various strategies have been employed to deal with these issues. Most commonly, probes are built to be robust and are constructed of materials that can withstand cleaning, sterilizing and autoclaving. Another strategy is through the use of a disposable protective sheath. Considerations must be taken to use sheath materials that will not interfere with the Raman measurements.

A real breakthrough would be achieved by the production of single-use probes. By far the greatest limitation in constructing disposable probes is the high cost of optical filters and assembly. The group of Popp has designed a probe using integrated fibre Bragg gratings and multiple multicore single mode fibres in the collection that could potentially be disposable, as these fibres can eventually be cheaply made without the requirement of relatively expensive additional optical filter components.[46] Alternatively, our own research group has developed a probe of fused silica fibres inside of a single use hypodermic needle tip which connects to a reusable probe body where the expensive optics are located.[50]

Perturbation factors

External factors

Sample/patient preparation

Schleusener *et al* provides a comprehensive review of their study of the effects of different potential perturbation factors in a measurement with a biomedical Raman probe.[108] They found that sample preparation was one of the biggest sources of variance in Raman measurements on the skin: factors like body hair, skin creams, and lotions had a significant effect on the resulting spectra.

Ambient light

Ambient light has a considerable influence on Raman spectra taken in the clinical environment. Standard fluorescent or luminescent bulbs contribute mercury emission lines or broadband light respectively, as significant artefacts in the Raman spectrum. Taking measurements in a clinic or during surgery in a completely dark environment is not always possible, so one way to overcome this is by using LED lights, which typically have a much smaller contribution to the near infrared spectral background.[65,102]

Conclusions

Raman spectroscopy has been demonstrated to be a powerful diagnostic platform technology. *In vivo* probes show great promise for clinical use, but important design considerations must be made for each possible biomedical application. Here we have outlined various methods whereby Raman probes can be tailored depending on the clinical need; particularly the accessibility of the tissues, the sample size and structure, required sampling depth, and significance of the difference in the Raman spectral signals between the sample groups of interest.

Acknowledgements

The authors wish to thank the National Institute of Health Research (UK) for their support of this work.

Notes and references

1 I. Latka, S. Dochow, C. Krafft, B. Dietzek and J. Popp. *Laser Photonics Rev* 2013, **7**(5):698-731.

2 U. Utzinger and R. R. Richards-Kortum. *J Biomed Opt, 2003,* 8(1):121-147.

3 Choo-Smith, L-P., et al. *Biopolymers* 67.1 (2002): 1-9.

4 K. Kong, C. Kendall, N. Stone, I. Notingher, Advanced Drug Delivery Reviews, 2015, **89**, 121–134.

5 C. Kendall, M. Isabelle, F. Bazant-Hegemark, J. Hutchings, L. Orr, J. Babrah, R. Baker, N. Stone. *Analyst,* 2009, **134**, 1029-1045.

6 C.V. Raman, *Nature, 1928,* **121**, 501-502.

7 N. Stone, C. Kendall, J. Smith, P. Crow and H. Barr*, Faraday Discuss.*, 2004, **126**: 141-157.

8 C. Kendall, N. Stone, N. Shepherd, K. Geboes, B. Warren, R. Bennett and H. Barr. *J. Path.* 2003, **200**(5):602-609

9 P Crow, B Barrass, C Kendall, M Hart-Prieto, M Wright, R Persad, N Stone, *British Journal of Cancer,* 2005, 92 (12), 2166-2170.

10 M Sattlecker, R Baker, N Stone, C Bessant, *Chemometrics and Intelligent Laboratory Systems*, 2011, **107** (2), 363-370.

11 Lloyd GR, Almond LM, Stone N, Shepherd N, Sanders S, et al. *Analyst*, 2014, **139**, 381-388.

12 P Crow, JS Uff, JA Farmer, MP Wright, N Stone, *BJU international*, 2004, **93** (9), 1232-1236.

13 C.A. Lieber, E. H. E. Nethercott, M.H. Kabeer, Biomedical Optics Express, 2010, **1**, 3, 975.

14 SP, Singh, A. Sahu, A. Deshmukh, P. Chaturvedi, C.M. Krishna, *Analyst*, 2013, **138** (14), 4175-82, doi: 10.1039/c3an36761d.

15 M. Miyagi, S. Kawakami,. *J. Lightwave Technol* 1984, **2**(2), 116-126

16 M. Miyagi. *J Lightwave Technol* 1985, **3**(2),303-307.

17 Y. Komachi, H. Sato, K. Aizawa, H. Tashiro, *Applied Optics,* 2005, **44**(22):4722-4732.

18 Y. Komachi, H. Sato, Y. Matsuura, M. Miyagi, and H. Tashiro. *Optics Letters*, 2005, **30**(21), 2942-2944.

19 J. Ma and Y.-S. Li, *Applied Spectrosc*. 1994, **48**(12),1529-1531.

20 J. Ma and Y.-S. Li. *Applied Optics,* 1996, **35**(15), 2527-2533.

21 M.G. Shim and B.C. Wilson, *Journal of Raman Spectroscopy* 1997, **28**(2-3),131–142.

22 M. G. Shim, B. C. Wilson, E. Marple, and M. Wach. *Appl. Spectrosc,* 1999, **53**(6), 619-627.

23 A. Mahadevan-Jansen, M. Follen Mitchell, N. Rarnanujam, U. Utzinger, and R. Richards-Kortum, *Photochemistry and Photobiology*, 1998, **68**(3): 427-431.

24 J. T. Motz, M. Hunter, L. H. Galindo, J. A. Gardecki, J. R. Kramer, R. R. Dasari, and M. S. Feld, *Applied Optics*, 2004, **43**(3), 542-554.

25 M. V. Schulmerich, K. A. Dooley, M. D. Morris, T. M. Vanasse, S. A. Goldstein, *J. Biomed. Opt*. 2006, **11**(6), 060502.

26 M. V. Schulmerich, W. F. Finney, V. Popescu, M. D. Morris, T. M. Vanasse, S. A. Goldstein., *Proc. SPIE **6093**; Biomedical Vibrational Spectroscopy III: Advances in Research and Industry*, 2006.

27 P. Matousek, E. R. C. Draper, A. E. Goodship, I. P. Clark, K. L. Ronayne, and A. W. Parker, *Appl. Spectrosc*., 2006**, 60**(7),758-763.

28 Y. Hattori, Y. Komachi, T. Asakura, T. Shimosegawa, G.-I. Kanai, H. Tashiro, and H. Sato. *Appl. Spectrosc*, 2007, **61**(6),579-584.

29 J. C. C. Day, R. Bennett, B. Smith, C. Kendall, J. Hutchings, G. M. Meaden, C. Born, S. Yu and N. Stone. *Phys. Med. Biol.* 2009, **54**(23), 7077.

30 C. Kendall, J. C. C. Day, J. Hutchings, B. Smith, N. Shepherd, H. Barr and N. Stone*, Analyst*, 2010, **135**, 3038-3041.

31 L. M. Almond, J. Hutchings, C. Kendall, J. C. C. Day, O. A. C. Stevens, G. R. Lloyd, N. A. Shepherd, H. Barr, N. Stone. *J. Biomed. Opt.* 2012, **17**(8), 081421

32 N. D. Magee, J. S. Villaumie, E. T. Marple, M. Ennis, J. S. Elborn and J. J. McGarvey *J. Phys. Chem. B*, 2009, **113**(23), 8137–8141.

33 C. Matthäus, S. Dochow, G. Bergner, A. Lattermann, B. F. M. Romeike, E. T. Marple, C. Krafft, B. Dietzek, B. R. Brehm, and J. Popp. *Anal. Chem*. 2012**, 84**, 7845−7851.

34 M. Sharma, E. Marple, J. Reichenberg, and J. W. Tunnell., *Rev. Sci. Instrum*. 2014, **85**, 083101.

35 J. Desroches, M. Jermyn, K. Mok, C. Lemieux-Leduc, J. Mercier, K. St-Arnaud, K. Urmey, M.-C. Guiot, E. Marple, K. Petrecca, and F. Leblond. *Biomedical Optics Express* 2015, **6**(7), 2380-2397.

36 M. Agenant, M. Grimbergen, R. Draga, E. Marple, R. Bosch, and C. van Swol, *Biomedical Optics Express*, 2014, **5**(4), 1203-1216.

37 M. Jermyn, K. Mok, J. Mercier, J. Desroches, J. Pichette, K. Saint-Arnaud, L. Bernstein, M.-C. Guiot, K. Petrecca and F. Leblond. *Cancer Imaging, Sci Trans Med,* 2015, **7**(274): 274ra19.

38 M. D. Keller, S. K. Majumder, and A. Mahadevan-Jansen. *Optics Letters*, 2009, **34**(7), 926-928.

39 M. D. Keller, E. Vargis, N. de Matos Granja, R. H. Wilson, M.-A. Mycek, M. C. Kelley, A. Mahadevan-Jansen *J. Biomed. Opt. 2011* **16**(7): 077006.

40 T. Katagiri, Y. S. Yamamoto, Y. Ozaki, Y. Matsuura, and H. Sato, *Appl. Spectrosc.* 2009, **63**(1), 103-107.

41 F. W. L. Esmonde-White, K. A. Esmonde-White, M. D. Morris. *Proc. SPIE 7548, Photonic Therapeutics and Diagnostics VI, **75484D,*** 2010.

42 P. I. Okagbare, F. W. L. Esmonde-White, S. A. Goldstein and M. D. Morris. *Analyst*, 2010, 135, 3142–3146.

43 M. S. Bergholt, W. Zheng, K. Lin, K. Y. Ho, M. Teh, K. G. Yeoh, J. B. Y. So, Z. Huang, *Technol Cancer Res Treat,* 2011, **10**(2) 103-112.

44 J. Wang, M. S. Bergholt, W. Zheng, Z. Huang. *Optics Letters*, 2013, **38**(13): 2321.

45 M. S. Bergholt, W. Zheng, K. Y. Ho, M. The, K. G. Yeoh, J. B. Y. So, A. Shabbir, and Z. Huang. *Gastroenterology in Motion*, 2014,**4**(146):27-32.

46 S. Dochow, I. Latka, M. Becker, R. Spittel, J. Kobelke, K. Schuster, A. Graf, S. Brückner, S. Unger, M. Rothhardt, B. Dietzek, C. Krafft, and J. Popp. *Optics Express*, 2012, **20** (18), 20156-20169.

47 S.O. Konorov, C. Addison, H.G. Schultz, R.F.B. Turner, M.W. Blades, *Optics Letters*, 2006, **31**, 12; 1911-1913.

48 P. Ghenuche, S. Rammler, N. Y. Joly, M. Scharrer, M. Frosz, J. Wenger, P. St. J. Russell, and H. Rigneault, *Optics Letters*, 2012, **37**(21), 4371-4373.

49 P.I. Okagbare, M. D. Morris*, Appl. Spectrosc.* 2012, **66**(6), 728-730.

50 J.C.C. Day and N. Stone. *Appl. Spectrosc.*, 2013, **67**(3): 349-354.

51 F. W. L. Esmonde-White and M. D. Morris. *Proc. SPIE 8565, Photonic Therapeutics and Diagnostics IX, 85656K*, 2013.

52 Kaiser Optical Systems, www.Kosi.com

53 Z. Huang, M.S. Bergholt, W. Zheng, K. Lin, K.Y. Ho, M. Teh, K.G. Yeoh, *Journal of Biomedical Optics* 15, no. 3 (2010): 037017-037017.

54 J. Mo, W. Zheng, H. Zhiwei. *Biomedical Optics Express,* 2010, 17-30.

55 O. A. C. Stevens, J. Hutchings, W. Gray, J.C.C. Day; Proc. SPIE 8939, Biomedical Vibrational Spectroscopy VI: Advances in Research and Industry, 89390W (March 4, 2014).

56 Z. Wang, H. Ding, G. Lu, and X. Bi. *Optics Letters*, 2014, **39**(13).

57 I.E. Iping Petterson, J.C.C. Day, L. Fullwood, B. Gardner, N. Stone *Analytical and bioanalytical chemistry*, 2015, **407** (27), 8311-8320.

58 J. Smith, C. Kendall, A. Sammon, J. Christie-Brown, N. Stone, *Technol. Cancer Res. Treat.*,2003, **2**, 327-331.

59 J. Horsnell, P. Stonelake, J. Christie-Brown, G. Shetty, J. Hutchings, C. Kendall, N. Stone, *Analyst*, 2010, **135,** 3042-3047.

60 A.S. Haka, Z. Volynskaya, J.A. Gardecki, J. Nazemi, R. Shenk, N. Wang, R.R. Dasari, M. Fitzmaurice, M.S. Feld, J. Biomed. Opt., 2009, **14**.

61 P. Matousek and N. Stone *Chem. Soc. Rev*., 2015, DOI: 10.1039/C5CS00466G.

62 S. Koljenovic, T.C.B. Schut, R. Wolthuis, A.J.P.E. Vincent, G. Hendriks-Hagevi, L. Santos, J.M. Kros, G.J. Puppels, *Anal. Chem.*, 2007, **79,** 557-564.

63 L.F. Santos, R. Wolthuis, S. Koljenovic, R.M. Almeida, G.J. Puppels, Anal. Chem., 2005, **77**, 6747-6752.

64 S. Koljenovic, T.C.B. Schut, R. Wolthuis, B. de Jong, L. Santos, P.J. Caspers, J.M. Kros, G.J. Puppels, *J. Biomed. Opt.,* 2005, **10**.

65 C.A. Lieber, S.K. Majumder, D.L. Ellis, D.D. Billheimer, A. Mahadevan-Jansen, *Lasers in Surgery and Medicine*, 2008, **40**, 461-467.

66 H. Lui, J. Zhao, D.I. McLean, H. Zeng, *Cancer Research*, 2012, **72**.

67 M.G., Shim, L.M. Song, N.E, Marcon, B.C. Wilson, *Photochem Photobiol*., 2000, **72** , 1, 146-50.

68 J.T. Motz, S.J. Gandhi, O.R. Scepanovic, A.S. Haka, J.R. Kramer, R.R. Dasari, M.S. Feld, *J Biomed Opt.*, 2005, **10 ,** 3, 031113.

69 L.M. Wong Kee Song, A. Molckovsky, K.K. Wang, L.J. Burgart, B. Dolenko, R.J. Somorjai, B.C. Wilson, Proc. of SPIE, 5692, 2005 140—146.

70 M.S. Bergholt, W. Zheng, K. Lin, K.Y. Ho, M. The, K.G. Yeoh, J.B. So, Z. Huang, *Analyst*, 2010, **135**, 12, 3162-8.

71 E. Widjaja, W. Zheng, Z. Huang, *International Journal of Oncology*, 2008, **32** ,653-662.

72 A. Taketani, R. Hariyani, M. Ishigaki, B.B. Andriana, H. Sato, *Analyst*, 2013, **138**, 4183-4190.

73 M.A. Short, I.T. Tai, D. Owen, H. Zeng, *Optics Express*, 2013, **21**, 5025-5034.

74 T.C. Bakker Schut, M.J. Witjes, H.J. Sterenborg, O.C. Speelman, J.L. Roodenburg, E.T. Marple, H.A. Bruining, G.J. Puppels, *Anal. Chem.*, 2000, **72**, 6010-6018.

75 L.-M. Wong Kee Song, B.C. Wilson, *Clinical gastroenterology*, 2005, **19**, 833-856.

76 S.K. Teh, W. Zheng, K.Y. Ho, M. Teh, K.G. Yeoh, Z. Huang, *Br. J. Cancer*, 2008, **98**, 457-465.

77 L.M. Almond, J. Hutchings, G. Lloyd, H. Barr, N. Shepherd, J. Day, O. Stevens, S. Sanders, M. Wadley, N. Stone, C. Kendall, *Gastrointestinal Endoscopy*, 2014, **79**, 37-45.

78 P. Crow, A. Molckovsky, N. Stone, J. Uff, B. Wilson, L.M. Wongkeesong, Urology, 2005, **65**, 6, 1126-1130.

79 M.C.M. Grimbergen, C.F.P. Van Swol, R.O.P. Draga, P. Van Diest, R.M. Verdaasdonk, N. Stone, et al., *Progress in Biomedical Optics and Imaging*–Proceedings of SPIE 2009, 7161.

80 M.A. Short, S. Lam, A.M. McWilliams, D.N. Ionescu, H. Zeng, *Journal of Thoracic Oncology*, 2011, **6**, 1206-1214.

81 M.C.M Grimbergen, C.F.P. van Swol, R.J.A. van Moorselaar, J. Uff, A. Mahadevan-Jansen, N. Stone, *Journal of Photochemistry and Photobiology B: Biology,* 2009 **95**, 3, 170—6.

82 R. Cicchi, A. Cosci, S. Rossari, D. Kapsokalyvas, E. Baria, V. Maio, D. Massi, V. De Giorgi, N. Pimpinelli, F.S. Pavone, *J. Biophotonics,* 2014, **7**, 86–95.

83 S. Dochow, D. Ma, I. Latka, T. Bocklitz, B. Hartl, J. Bec, H. Fatakdawala, E. Marple, K. Urmey, S. Wachsmann-Hogiu, M. Schmitt, L. Marcu, J. Popp, *Anal Bioanal Chem*, 2015, **407**, 8291–8301.

84 M. Nyberg, V. Jalkanen, K. Ramser, B. Ljungberg, A. Bergh & O. A. Lindahl, *Journal of Medical Engineering & Technology*, 2015, **39**, 3, 198-207.

85 K. A. Esmonde-White, F. W. L. Esmonde-White, M. D. Morris and B. J. Roessler. *Analyst*, 2011, **136**, 1675.

86 J. T. Meade, B. B. Behr, Y. Bismilla, A. T. Cenko, Brandon DesRoches, A. Henkin, E. A. Munro, J. Slaa, S. Baker, D. Rempel, A. R. Hajian, Proc. SPIE 8982, Optical Components and Materials XI, 898222 2014.

87 O. A. Stevens, 'Miniature Raman probes for medical applications', Doctoral Dissertation, University of Bristol, 2015

88 De Jong, Bas WD, Tom C. Bakker Schut, Kees Maquelin, Theo Van Der Kwast, Chris H. Bangma, Dirk-Jan Kok, and Gerwin J. Puppels. *Analytical chemistry* 78, no. 22 (2006): 7761-7769.

89 J. Mo, W. Zheng, J. J. H. Low, J. Ng, A. Ilancheran and Z. Huang, *Anal Chem*., 2009, **81**(21), 8908–8915

90 H. Sato, Y. S. Yamamoto, A. Maruyama, T. Katagiri, Y. Matsuura, Y. Ozaki, *Vib. Spectrosc.* 2009, **50**(1), 125–130.
91 Komachi, Yuichi, Takashi Katagiri, Hidetoshi Sato, and Hideo Tashiro. *Applied optics* 48, no. 9 (2009): 1683-1696.
92 T. F. Cooney, C. L. Schoen, S. K. Sharma, D.M. Carey, *Appl Spectrosc*, 1993, **47**(10):1683-1692.
93 G. Shetty, C. Kendall, N. Shepherd, N. Stone and H. Barr, *British Journal of Cancer*, 2006, **94**, 1460–1464
94 M. G. Shim, B. C. Wilson, E. Marple, M. L. Wach, *Proc. SPIE 3257, Infrared Spectroscopy: New Tool in Medicine*, 1998, **208.**
95 F. Jaillon, W. Zheng, and Z. Huang. *Phys. Med. Biol*. 2008, **53**, 937.
96 P. Matousek, I.P. Clark, E.R.C. Draper, M.D. Morris, A.E. Goodship, N. Everall, M. Towrie, W.F. Finney, and A.W. Parker. *Appl. Spectrosc*. 2005**,** 59(4):393-400.
97 P. Matousek and N. Stone. *J Biophotonics, Special Issue: Vibrational Spectroscopy in Medicine*, 2013, **6**(1),7–19.
98 I. E. Iping Petterson, P. Dvořák, J. B. Buijs, C. Gooijer and F. Ariese. *Analyst*, 2010,**135**, 3255-3259.
99 K. Buckley and P. Matousek, *Analyst*, 2011, **136**, 3039-3050.
100 N.Stone and P. Matousek, *Cancer Research*, 2008, **68** (11), 4424-4430.
101 M. Z. Vardaki, B. Gardner, N. Stone and P. Matousek, *Analyst*, 2015, **140,** 5112-5119.
102 MM Kerssens, P Matousek, K Rogers, N Stone, *Analyst*, 2010, **135** (12), 3156-3161.
103 Harris, Andrew T., Andrew Rennie, Haroon Waqar-Uddin, Sarah R. Wheatley, Samit K. Ghosh, Dominic P. Martin-Hirsch, Sheila E. Fisher, Alec S. High, Jennifer Kirkham, and Tahwinder Upile. *Head & neck oncology* 2, no. 1 (2010): 26.
104 Skinner, H. Trey, Thomas F. Cooney, S. K. Sharma, and S. M. Angel. *Applied spectroscopy* 50, no. 8 (1996): 1007-1014.
105 H. R. Morris, C. C. Hoyt, and P. J. Treado, *Appl. Spectrosc.,* 1994, **48**(7), 857-866.
106 H. R. Morris, C. *C. Hoyt, P. Miller, and P. J. Treado, Appl. Spectrosc,* 1996, **50**(6),805-811.
107 N. Stone *'Raman spectroscopy of biological tissue for application in optical diagnosis of malignancy.'* Doctoral Dissertation, Cranfield University, 2001.
108 J. Schleusener, P. Gluszczynska, C. Reble, I. Gersonde, J. Helfmann, H.-J. Cappius, J. W. Fluhr, M. C. Meinke. *Appl Spectrosc*, 2015, **69(**2): 243-256.